Fault-Tolerant Current Control of Six-Phase Permanent Magnet Motor With Multifrequency Quasi-Proportional-Resonant Control and Feedforward Compensation for Aerospace Drives

Jinquan Xu, *Senior Member, IEEE*, Si Guo, *Student Member, IEEE*, Hong Guo, *Senior Member, IEEE*, and Xinlei Tian, *Student Member, IEEE*

***Abstract*— To improve the current tracking performance, this article proposes a new fault-tolerant current control for the six-phase fault-tolerant permanent magnet synchronous motor (FTPMSM) system with multifrequency quasi-proportional-resonant (QPR) control and back electromotive force (EMF) feedforward compensation, which can track the time-varying sinusoidal and nonsinusoidal reference currents in the stationary reference frame (SRF) under normal and fault conditions. First, the multifrequency QPR current controller with shunt topology is proposed to track the time-varying reference current in SRF, which can guarantee the current control performance regardless of the motor speed variation and the load torque change. Second, the optimized feedforward compensation method for the back EMF is proposed to further reduce the steady-state current tracking error, which takes the time delay of the digital implementation into consideration. Finally, the effectiveness of the proposed approach is verified on a 3 kW six-phase FTPMSM platform. The resulting six-phase FTPMSM system with the proposed current control has great current tracking performance, strong robustness to various external/internal disturbance, as well as low computational burden, which can guarantee the multiphase FTPMSM system performance in normal and fault conditions.**

***Index Terms*—Current control, fault tolerant motor, permanent magnet motor, quasi-proportional-resonant control.**

Manuscript received 20 January 2022; revised 4 April 2022 and 10 July 2022; accepted 27 August 2022. Date of publication 30 August 2022; date of current version 10 October 2022. This work was supported in part by the National Natural Science Foundation of China under Grant 52177028, in part byAeronautical Science Foundation of China under Grant 201907051002, in part bythe Fundamental Research Funds for the Central Universities under Grant YWF21BJJ522, and in part by Major Program of the National Natural Science Foundation of China under Grant 51890882. Recommended for publication by Associate Editor J. He. *Corresponding author: Hong Guo.)*

Jinquan Xu and Hong Guo are with the School of Automation Science and Electrical Engineering and the Science and Technology on Aircraft Control Laboratory, Beihang University, Beijing 100191, China, and also with the Ningbo Innovation Research Institute, Ningbo 315800, China (e-mail: xujinquan@buaa.edu.cn; guohong_buaa@163.com).

Si Guo is with the School of Automation Science and Electrical Engineering and the Science and Technology on Aircraft Control Laboratory, Beihang University, Beijing 100191, China, and also with the Beijing Institute of Mechanical Equipment, Beijing 100039, China (e-mail: guosi@buaa.edu.cn).

Xinlei Tian is with the School of Automation Science and Electrical Engineering and the Science and Technology on Aircraft Control Laboratory, Beihang University, Beijing 100191, China (e-mail: tianxinlei@buaa.edu.cn).

Color versions of one or more figures in this article are available at https://doi.org/10.1109/TPEL.2022.3202929.

Digital Object Identifier 10.1109/TPEL.2022.3202929

I. Introduction

DUE to high fuel efficiency, low emission, and good maintainability, the more-electric aircraft has brought a technological revolution in the aviation industry, which is characterized by the electrical systems fully or partially replacing the traditional on-board systems powered by hydraulic or pneumatic energies, such as the Boeing 787 and Airbus A380 [1], [2], [3]. The electrical machine is the key component of electromechanical energy conversion, which has been widely applied for the flight control, the braking system, and the fuel pump [4], [5]. To guarantee the flight safety, the high reliability electrical machine system has attracted much attention in the more-electric aircraft field [6], [7], [8].

The fault-tolerant permanent magnet synchronous motor (FTPMSM) has a simple structure, high power density, and strong fault tolerance, which is very suitable for the more-electric aircraft application [9], [10], [11]. The FTPMSM system makes use of the multiple single-phase winding to improve the reliability, which can operate continuously in fault condition by the fault-tolerant control of the remaining nonfault phase windings. To improve the fault-tolerant performance, considerable efforts have been conducted on the fault-tolerant control of the FTPMSM system to generate the nonfault current references [12]. In [13], the optimal torque control (OTC) is proposed to output the constant torque of the FTPMSM by minimizing the total copper loss, in which the nonfault current references consist of numerous high-order harmonics. To solve this issue, in [14], the third harmonic current injection-based fault-tolerant control is proposed to guarantee the phase open-circuit fault-tolerant operation. However, the nonfault current references are not optimized. In [15], the fault-tolerant control by reconfiguring maximum round magnetomotive force is proposed for the FTPMSM system in phase open-circuit fault condition, in which the nonfault current references are still sinusoidal. But this method can not eliminate the electromagnetic torque ripple. Due to simple structure, low computation burden and easy realization, the OTC has been widely applied for the fault-tolerant control of the FTPMSM system. Note that to guarantee the fault-tolerant performance of the FTPMSM system in fault condition, the nonfault current references are usually time-varying and

nonsinusoidal, which add the difficulty for the current tracking control. To solve this issue, considerable efforts have been made on the current control for the FTPMSM system. In [16] and [17], the hysteresis current control is proposed to guarantee the phase current tracking performance of the FTPMSM system. It has a simple structure, low computation burden, and good robustness to the system parameter variation. But the hysteresis current control can result in serious subharmonic current components due to the varying switching frequency, which will cause the system performance degradation. To deal with the issue associated with the varying switching frequency, the current control in a synchronous frame is proposed by the improved coordinate transformation, which has an excellent steady-state control performance. But this method has poor dynamic performance, which cannot achieve the current tracking with high harmonics [18], [19]. In [20], [21], [22], [23], the model predictive current control is proposed to guarantee the fault-tolerant performance of the FTPMSM system, which is an optimum control with fast response. But it is extremely sensitive to the system parameter variation. To enhance the robustness, the proportional-resonant-based current control is proposed for the FTPMSM system under phase open-circuit and short-circuit fault conditions [24]. But this method can only guarantee excellent current tracking performance around the resonance frequency with a high computation cost, in which the variable speed drive performance can not be guaranteed. In [25], a new feedforward current control is proposed to improve the transient current control performance, which has the advantage of simple implementation and good robustness. But this method cannot be applied for the current tracking control in stationary reference frame. Furthermore, the back EMF can also cause the current tracking performance degradation, which cannot be addressed by the abovementioned methods. Therefore, the high performance current control of the FTPMSM system in fault condition has not received much attention and remains a challenging problem.

Motivated by this, a new fault-tolerant current control with multifrequency QPR control and back EMF feedforward compensation is proposed for the six-phase FTPMSM system, which can track the time-varying sinusoidal and nonsinusoidal reference current in SRF in full-speed range. The main contributions of this article are fourfold. First, the multifrequency QPR current control with shunt topology is proposed, which can guarantee the time-varying sinusoidal/nonsinusoidal current tracking performance with almost no steady error around the resonance frequency. This distinguish the current research from the existing phase current tracking methods. Second, the parameter design criteria of the QPR current controller is proposed including the resonant frequency, the proportional coefficient, and the resonant coefficient, which can guarantee the current control performance in full-speed range. Third, the optimized feedforward compensation is proposed considering the time delay of the digital implementation, which can compensate the current control performance degradation caused by the back EMF. It was not available earlier. Fourth, the effectiveness of the proposed current control is verified on a 3 kW six-phase FTPMSM platform. The resulting FTPMSM system with the proposed current control has an excellent fault-tolerant performance and strong robustness to various disturbances with low computational burden in the full-speed range.

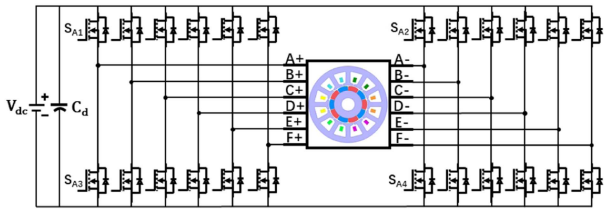

Fig. 1. Six-phase FTPMSM system.

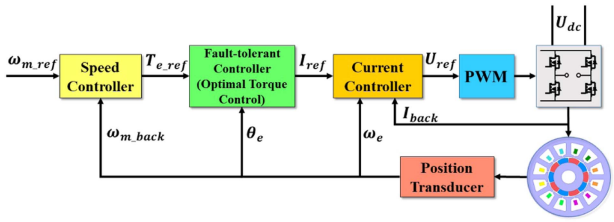

Fig. 2. Dual closed loop control scheme.

The rest of this article is organized as follows. In Section II, the multifrequency QPR-based current control scheme with back EMF feedforward compensation is proposed for the FTPMSM system. In Section III, the multifrequency QPR current control design is presented. The back EMF feedforward compensation is introduced in Section IV. The experimental results on the six-phase FTPMSM system are given in Section V, while Section VI concludes this article.

II. FTPMSM Control Scheme

Due to the outstanding fault-tolerant performance, the six-phase FTPMSM adopts the 10-pole/12-slot symmetrical structure with the alternate-teeth-wound single-layer windings, which has been widely applied in safety-critical field. Furthermore, each phase is powered by a single H-bridge-type inverter as shown in Fig. 1. Compared with the traditional two-level six-bridge inverter, the H-bridge-type inverter has prominent superiority in fault isolation and fault tolerance. The dual closed control scheme is adopted for the FTPMSM system as shown in Fig. 2. In addition, the optimal torque control (OTC) is adopted to calculate each phase current command, which can guarantee the no-ripple torque output performance of the system even in fault condition [13], [26]. The current control is used to ensure the time-varying phase current tracking performance, which will be introduced in next section. The main specification and parameters of the FTPMSM system are listed in Table I.

For the six-phase FTPMSM, the electromagnetic torque can be expressed as

$$T_{em} = \sum_{i \in \Psi} K_i I_i, \quad \text{for } \Psi = \{A, B, C, D, E, F\} \tag{1}$$

TABLE I
SPECIFICATION OF THE FTPMSM SYSTEM

Parameters [Unit]	Value
DC bus voltage [V]	160
Rated speed [rpm]	3000
Rated torque [N·m]	10
Phase resistance [Ω]	0.055
Phase inductance [mH]	1.14
Switching frequency [kHz]	20

with

$$K_i = K_M \sin(\omega_e t + \theta_i), \quad \text{for } \theta_i \in \left\{0, \frac{\pi}{3}, \frac{2\pi}{3}, \pi, \frac{4\pi}{3}, \frac{5\pi}{3}\right\} \tag{2}$$

where T_{em} denotes the electromagnetic torque, K_i, I_i denote the ith phase back EMF coefficient and current, K_M denotes the maximum phase back EMF coefficient. In addition, ω_e and θ_i denote the electrical angular velocity and phase angle.

After the fault occurrence, the electromagnetic torque of the FTPMSM can be expressed as

$$T_{em} = \sum_{i\in\Psi_n} K_i I_i + \sum_{j\in\Psi_f} K_j I_j = T_{en} + T_{ef} \tag{3}$$

where Ψ_n and Ψ_f denote the set of the nonfault and fault phase, T_{en} and T_{ef} denote the electromagnetic torque component generated by the nonfault and fault phase.

The OTC is an optimized fault-tolerant control by converting the nonfault phase current solving problem into an constrained optimization problem, which can be expressed as

$$\min R \sum_{i\in\Psi_n} I_i^2 \tag{4}$$

with the constraint condition (3). Here, R denotes the phase resistance.

By the lagrange multiplier method, the nonfault phase current can be calculated as [27]

$$I_j = \frac{(T_{em} - T_{ef}) K_M \sin(\omega_e t + \theta_j)}{\sum_{i\in\Psi_n} K_M^2 \sin^2(\omega_e t + \theta_i)}. \tag{5}$$

Note that for the FTPMSM system with the OTC, by (5), the phase currents are all sinusoidal in normal condition, while the nonphase phase currents are nonsinusoidal containing numerous harmonics in phase open-circuit (POC) and phase short-circuit (PSC) fault conditions. In order for the phase current control, the harmonic analysis of the nonfault phase currents for the FTPMSM in fault-tolerant operation is conducted as shown in Fig. 3. In fault-tolerant condition, the nonfault phase currents contain mainly the first, third, and fifth harmonic components, which are also different with each nonfault phase. Compared with the first and third harmonic components, the amplitude of the fifth harmonic component is very small, which can be neglected. Note that as the increase of the controlled harmonic current components, the computational burden and the control

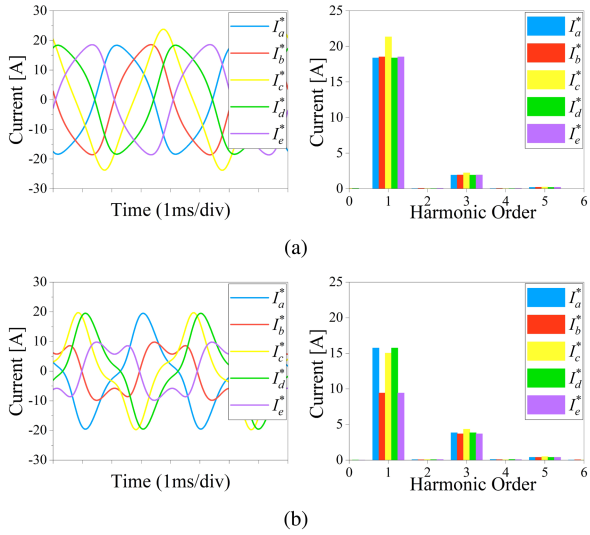

Fig. 3. Harmonic analysis of nonfault phase currents in F-phase fault condition. (a) In POC fault with 3000 r/min and 8 N · m. (b) In PSC fault with 3000 r/min and 5 N · m.

complexity of the FTPMSM system will significantly increase. By comprehensive consideration of control performance, computation burden, and practical engineering implementation, the first and third harmonic current components are used for the current tracking control of the FTPMSM system. In addition, there inevitably exists the back EMF variation in the phase current control, which can be considered as a disturbance for the control current. As a result, the high-order harmonics, unbalance, and back EMF disturbance bring the severe challenge for the phase current control of the FTPMSM system. To solve this issue, a new fault-tolerant current control with multifrequency QPR control and back EMF feedforward compensation is proposed for the FTPMSM system, which will be introduced in the next sections.

III. MULTIFREQUENCY QPR CURRENT CONTROL

Due to the simple structure and low computation burden, the PID control has been widely applied for the current control of the three-phase permanent magnet motor system. But the PID control has a narrow frequency bandwidth, which can only guarantee the no steady-state error control of the dc signal. Therefore, the traditional three-phase permanent magnet motor system usually adopts the coordinate transformation to convert the ac phase currents into the dc signals in rotating synchronous frame. Then the PID control is used to control the dc current signals in rotating synchronous frame. However, for the FTPMSM system during fault-tolerant operation, the nonfault phase windings are in unsymmetrical operation condition, for which the coordinate transformation-based current control cannot be applied.

To solve this issue, the fault-tolerant current control with multifrequency QPR control and back EMF feedforward compensation is proposed for the FTPMSM system, which is shown in Fig. 4. The multifrequency QPR controller is proposed to

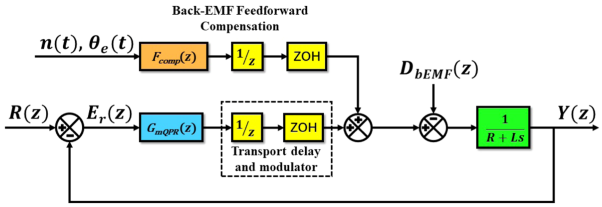

Fig. 4. Proposed current control scheme.

guarantee the sinusoidal and nonsinusoidal phase current tracking performance, while the back EMF forward compensation is proposed to eliminate the current tracking error due to the back EMF disturbance. Next, the multifrequency QPR controller will be designed.

A. Current Control Scheme

Due to the excellent tracking performance for the periodic time-varying signal, the QPR control has been widely applied in the variable speed electric drive field. By the harmonics analysis of the nonfault phase currents in fault-tolerant operation condition, the fundamental and third harmonic components of the phase current should be controlled to guarantee the fault-tolerant performance of the FTPMSM system. Therefore, the multifrequency QPR control is proposed for the current control of the FTPMSM system as follows:

$$G_{mQPR}(s) = K_p + \sum_{i=1,3,\ldots,n} \frac{2K_{ri}\omega_c s}{s^2 + 2\omega_c s + \omega_i^2} \tag{6}$$

where K_p denotes the proportional gain, K_{ri} and ω_i denote the ith harmonic resonant coefficient and resonant frequency, ω_c denotes the bandwidth of the QPR control. Note that the multifrequency QPR control can be considered as the superposition of multiple single-frequency QPR controllers, in which each QPR controller is used to control for a specified frequency harmonics.

In practical engineering, the proposed multifrequency QPR controller should be discretized to be implemented in the digital controller. But the QPR controller is sensitive to the discretization, which can cause the system performance degradation and even instability. To solve this issue, considerable efforts have been conducted on different discretization methods for the QPR controller. In this article, the binlinear transformation with frequency prewarping is adopted for the proposed multifrequency QPR control discretization, which can guarantee the control performance of the proposed controller even in high frequency applications. The bilinear transformation with frequency prewarping can be represented as

$$s = \frac{\omega_0}{\tan\left(\frac{\omega_0 T_s}{2}\right)} \cdot \frac{z-1}{z+1} \tag{7}$$

where T_s and ω_0 denote the sampling period and the resonant angular frequency, respectively.

With (7) in (6), the discretized multifrequency QPR controller can be represented as

$$G_{mQPR}(z) = K_p + \sum_{i=1,3,\ldots,n} \frac{K_{ri}b_i z^2 - K_{ri}b_i}{z^2 + a_{1i}z + a_{2i}} \tag{8}$$

with

$$a_{1i} = \frac{2\omega_i^2 - 2C_i^2}{C_i^2 + 2\omega_c C_i + \omega_i^2} \tag{9}$$

$$a_{2i} = \frac{C_i^2 - 2\omega_c C_i + \omega_i^2}{C_i^2 + 2\omega_c C_i + \omega_i^2} \tag{10}$$

$$b_i = \frac{2\omega_c C_i}{C_i^2 + 2\omega_c C_i + \omega_i^2} \tag{11}$$

$$C_i = \frac{\omega_i}{\tan\left(\frac{\omega_i T_s}{2}\right)}. \tag{12}$$

Note that the order n of the proposed multifrequency QPR control is associated with the operating condition of the FTPMSM system. The order n is set as 1 in normal condition, while the order n is set as 3 in fault-tolerant operating condition.

B. Control Parameter Design

To guarantee the current tracking performance with the proposed multifrequency QPR control (8), the control parameters ω_c, K_p, K_{r1}, and K_{r3} will be designed in this section. The design criterion for the control parameters can be summarized as follows.

1) The choice of ω_c should guarantee the proposed control with enough bandwidth at the resonant frequency.

2) The choice of K_p should guarantee both the stability and the transient response of the proposed control. That is, the magnitude response of the current closed-loop transfer function (CLTF) should approach to 0 dB and the frequency response should approach to 0° at the designated resonance frequency, which can be represented as

$$\begin{cases} 20\left(|CLTF|_{\omega=\omega_e}\right) \geq 0 \\ \angle CLTF_{\omega=\omega_e} \to 0^\circ \end{cases} \text{For normal condition} \tag{13}$$

$$\begin{cases} 20\left(|CLTF|_{\omega=3\omega_e}\right) \geq 0 \\ \angle CLTF_{\omega=3\omega_e} \to 0^\circ \end{cases} \text{For fault tolerant condition.} \tag{14}$$

3) The choice of K_{r1} and K_{r3} should guarantee that the proposed control can eliminate the steady-state errors of the phase and magnitude. Furthermore, the magnitude response of the CLTF with the proposed control at any high harmonic frequency should be far less than 0 dB to suppress the high harmonic current components, which can be represented as

$$\begin{cases} 20\left(|CLTF|_{\omega=3\omega_e,5\omega_e}\right) < 0 \text{ For normal condition} \\ 20\left(|CLTF|_{\omega=5\omega_e}\right) < 0 \qquad \text{For fault tolerant condition.} \end{cases} \tag{15}$$

4) Since the fundamental frequency of the phase current changes with the motor speed, the parameters of the proposed control should be applied in the whole operating speed range.

According to the characteristics of the QPR controller, the parameter ω_c is associated with the bandwidth at the resonant frequency. The increase of ω_c can increase the system bandwidth and decrease the dynamic response. Therefore, there exists a tradeoff for the choice of ω_c. Furthermore, to guarantee the enough bandwidth of the proposed control in the whole operating speed range, the parameter ω_c is selected as

$$\omega_c = 2\pi \cdot \frac{pn}{60} \cdot 1\% \tag{16}$$

where n denotes the motor speed and p denotes the pole pairs of the motor.

Since the proposed multifrequency QPR control performance is determined by the root locations of the CLTF characteristic polynomial, the root locus method is used for the design of K_p, K_{r1}, and K_{r3}. Fig. 5 shows the root loci of the CLTF with different K_p, K_{r1}, and K_{r3} at the rated frequency of 250 Hz. Note that with the increase of K_p, the poles p_1 and p_2 gradually move from the stable region within the unit circle to the outside of the unit circle (the unstable region), while the other two pairs of conjugate complex poles have almost no shift. As the increase of K_{r1}, the pole p_2 and the conjugate complex poles (p_3, p_3^*), (p_4, p_4^*) all move in the direction to the outside of the unit circle. And the conjugate complex poles (p_3, p_3^*) will reach the outside of the unit circle when $K_{r1} > 306$, which will result in the system instability. With the increase of K_{r3}, the corresponding poles have little change, while the conjugate complex poles (p_4, p_4^*) will move across the unit circle into the unstable region when $K_{r3} > 98$. Therefore, to guarantee the current tracking performance at the rated frequency of 250 Hz, the parameters of the proposed multifrequency QPR control should be satisfied as

$$\begin{cases} 0 < K_p < 18 \\ 0 < K_{r1} < 306 \\ 0 < K_{r3} < 98. \end{cases} \tag{17}$$

Similarly, the constraint condition of K_p, K_{r1}, and K_{r3} at different frequencies can be obtained. Finally, according to the system performance and the practical engineering experience, the control parameters are selected as $K_p = 2$, $K_{r1} = 100$, $K_{r3} = 10$.

C. Design Verification of the Proposed Current Controller

For the design verification, the Bode diagrams of the CLTF with the proposed multifrequency QPR control in normal and fault-tolerant operation conditions are shown as Fig. 6, in which two different resonant frequencies (50, 250 Hz) are applied.

Note that for the FTPMSM system in normal condition, there exists only one resonant frequency corresponding to the fundamental frequency. Furthermore, the closed-loop response with the proposed control can achieve the unit gain with almost no phase lag at the resonant frequency (50, 250 Hz). In addition, the closed-loop gains with the proposed control at the third and fifth harmonic frequencies are far less than 0 dB, which

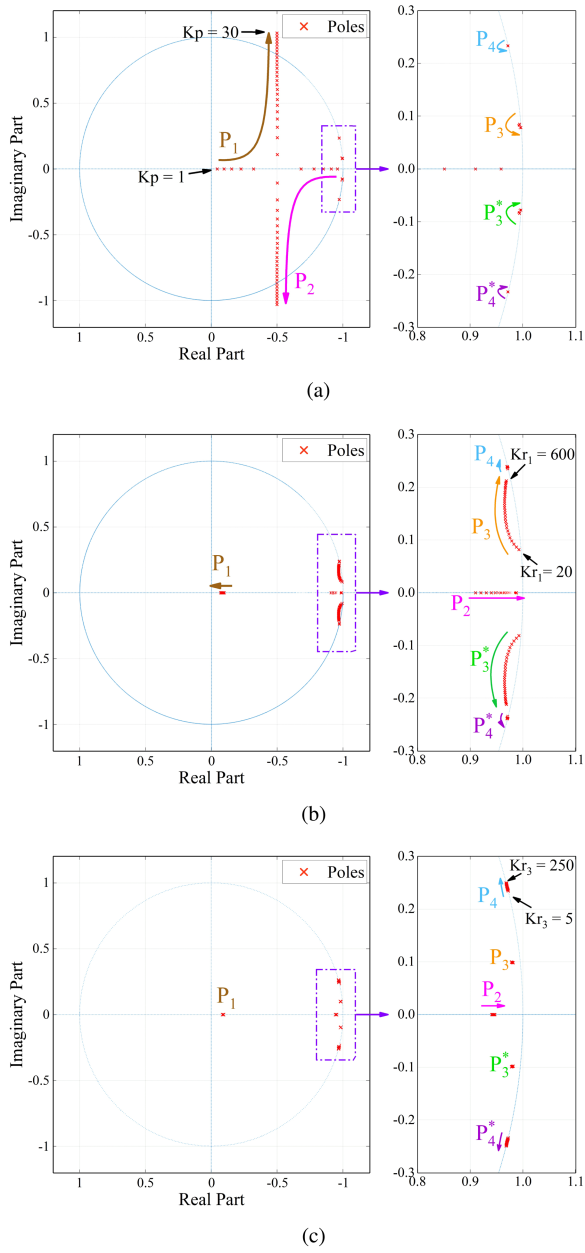

Fig. 5. Root loci of the CLTF with different K_p, K_{r1}, and K_{r3}.

implies that the proposed multifrequency QPR control can effectively suppress the high frequency interference signal in normal condition.

For the FTPMSM system in fault-tolerant operation condition, there are two resonant frequencies corresponding to the fundamental and third harmonics. And both the magnitude response and the phase response stay around zero at the fundamental and third harmonic frequencies. Therefore, the proposed multifrequency QPR control can guarantee the phase current tracking performance with no steady-state error in fault tolerant operation condition. Furthermore, as the closed-loop gains of the magnitude response at the fifth or higher harmonic frequencies are far less than 0 dB, the proposed multifrequency QPR control has the excellent suppression performance for the

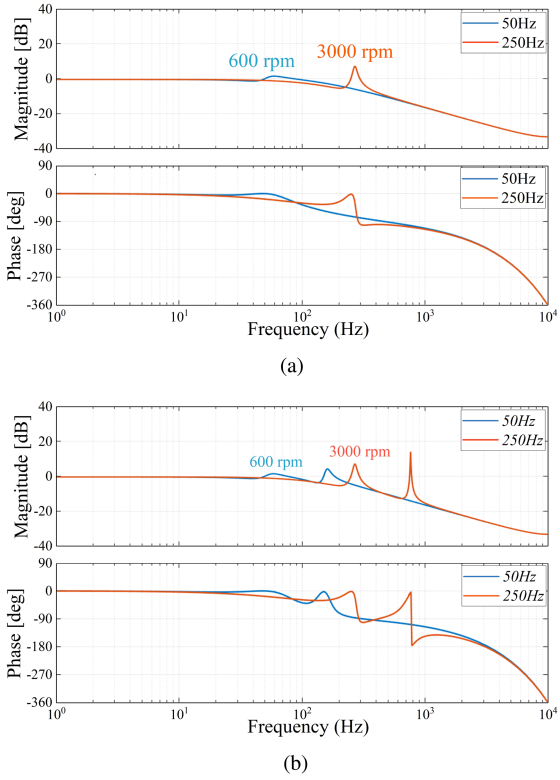

Fig. 6. Bode diagrams of the CLTF at 50 and 250 Hz.

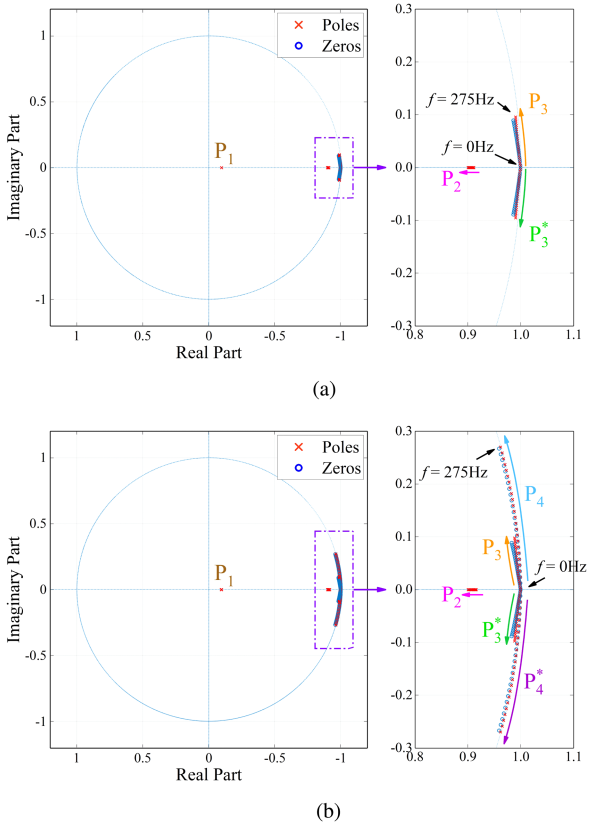

Fig. 7. Migration of the closed-loop poles and zeros in the whole operating frequency range from 0 to 275 Hz.

high frequency interference signal in fault-tolerant operation condition.

Since the resonant frequency changes with the motor speed, the closed-loop poles and zeros of the FTPMSM system will migrate with the operating frequency as well. To verify the effectiveness of the proposed current controller in the whole operating speed range, the root loci of the CLTF with the whole operating frequency range is shown in Fig. 7. Here, the motor speed range is taken from 0 to 3300 r/min (10% higher than the rated speed) by considering the speed ripple in practical engineering. Note that all the poles in the whole operating frequency range are located within the unit circle. Therefore, the proposed multifrequency QPR control can guarantee the current tracking performance of the FTPMSM system in the whole operating speed range under normal and fault-tolerant operation conditions.

To verify the robustness of the multifrequency QPR control to the motor parameter variations, the root loci of the CLTF with different phase resistance and inductance is shown in Fig. 8. Note that although the values of the phase resistance and inductance has varied more than 50% of their nominal values, all the poles in the whole operating frequency range are located within the unit circle. Therefore, the proposed multifrequency QPR control has the good robustness to the motor parameter variations.

Note that compared with the PR controller, although the gain in the resonant frequency decreases slightly, the proposed multifrequency QPR controller has better dynamic response

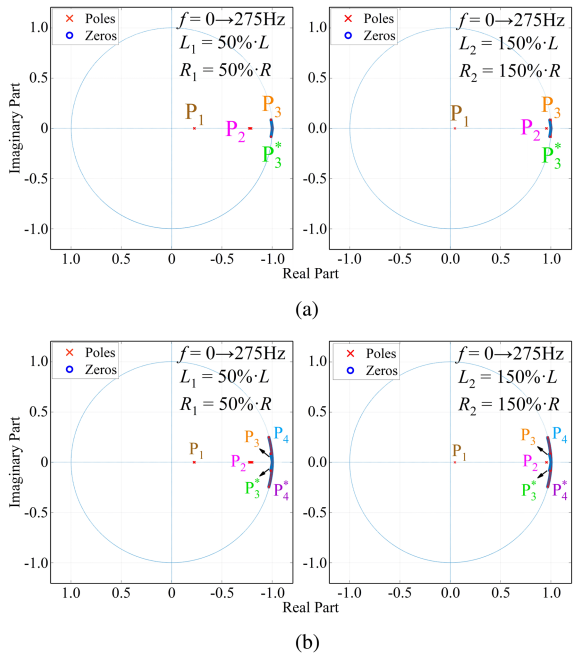

Fig. 8. Migration of the closed-loop poles and zeros with different phase resistance and inductance.

characteristic and current tracking control performance for the FTPMSM system in full speed region.

IV. Back EMF Feedforward Compensation

For the phase current control, the phase back EMF is time-varying and nonlinear, whose amplitude and frequency are proportional to the motor speed. Furthermore, when the motor operates under the high-speed light load condition, the phase back EMF is much larger than the current command, which will cause the current tracking performance degradation seriously. To solve this issue, a back EMF feedforward compensation method is proposed to eliminate the current tracking error due to the phase back EMF, which takes the time delay of the digital implementation into consideration.

According to the phase current control structure in Fig. 4, for the FTPMSM system without the back EMF feedforward compensation, the current tracking error $E(z)$ can be represented as

$$\begin{aligned} E(z) &= R(z)\frac{1}{1+G_{mQPR}(z)G_m(z)} \\ &\quad + D_{bEMF}(z)\frac{G_m(z)}{1+G_{mQPR}(z)G_m(z)} \\ &=: E_R(Z)+E_D(z) \end{aligned} \tag{18}$$

with

$$G_m(z) = \frac{1}{R}\cdot\frac{1-e^{-\frac{R}{L}T_s}}{z(z-e^{-\frac{R}{L}T_s})} \tag{19}$$

where $G_m(z)$ denotes the open-loop transfer function of the phase current in discrete domain and $E_D(z)$ denotes the current tracking error caused by the phase back EMF. Note that $E(z)\to 0$ as $G_{mQPR}(z)\to\infty$. However, due to the time delay of the digital implementation, the large gain of the proposed QPR control will cause the system instability. Therefore, the proposed multifrequency QPR control cannot eliminate the steady-state error $E_D(z)$ caused by the phase back EMF.

To enhance the current tracking performance, the back EMF feedforward compensation method is proposed, in which the current tracking error $E'(z)$ can be represented as

$$\begin{aligned} E'(z) &= R(z)\frac{1}{1+G_{mQPR}(z)G_m(z)} \\ &\quad + \frac{D_{bEMF}(z)G_m(z)-F_{comp}(z)G_m(z)}{1+G_{mQPR}(z)G_m(z)} \\ &=: E'_R(z)+E'_D(z). \end{aligned} \tag{20}$$

As a result, with the appropriate feedforward compensation term $F_{comp}(z)$, the current tracking error $E'_D(z)$ caused by the phase back EMF can be eliminated. By (2), the feedforward compensation term $F_{comp}(t)$ of the ith phase winding can be written as

$$F_{icomp}(t) = K_M\cdot n(t)\cdot\sin\left(\theta_e(t)+\theta_i\right) \tag{21}$$

where $n(t)$ denotes the rotor speed and $\theta_e(t)$ denotes the rotor electrical position. Note that the back EMF compensation is based on the measurement of $n(t)$ and $\theta_e(t)$. However, in practical engineering, there inevitably exists the time delay for the measurement of $n(t)$ and $\theta_e(t)$ due to the digital implementation as shown in Fig. 9, which decrease the feedforward compensation accuracy. To solve this issue, the effect of the time delay should be considered in the back EMF feedforward compensation.

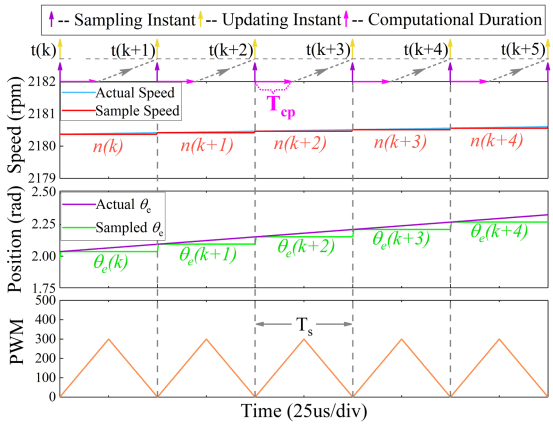

Fig. 9. Time sequence of rotor speed sampling, the rotor position sampling, PWM updating, and computational delay.

For the FTPMSM system, due to the existence of the moment of inertia, the motor speed change in one sampling period T_s can be neglected. That is

$$n(k+1)\approx n(k) \tag{22}$$

where k denotes the kth sampling period. Note that the motor speed change in one sampling period can be ignored mainly caused by the small sampling period. This means that the time derivative of speed may not be zero. Furthermore, the rotor electrical position in the $(k+1)$th sampling period can be represented as

$$\theta_e(k+1) = \theta_e(k)+\frac{2\pi}{60}\cdot n(k)\cdot p\cdot T_s. \tag{23}$$

Therefore, by (21) and (23), the feedforward compensation voltage $F_{comp}(t)$ of the ith phase winding in the $(k+1)$th sampling period with the time delay compensation can be represented as

$$F_{icomp}(k+1) = K_M\cdot n(k)\cdot\sin\left(\theta_e(k)+\frac{2\pi n(k)pT_s}{60}+\theta_i\right). \tag{24}$$

Note that the stability and the robustness of the proposed fault-tolerant current control is mainly guaranteed by the multifrequency QPR control, while the back EMF feedforward compensation is used to improve the phase current control performance. Compared with the traditional PR current control [28], the merits of the proposed current control are threefold. First, our proposed control is an universal time-varying nonsinusoidal phase current tracking control, rather than specific harmonic current component eliminating method, which can be applied more widely. Second, our proposed control can use the back

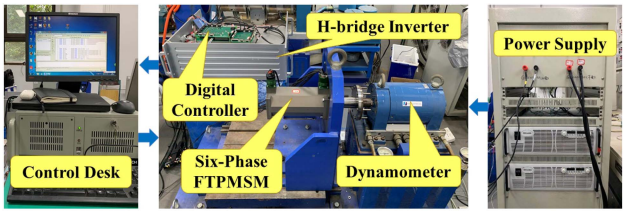

Fig. 10. FTPMSM experimental platform.

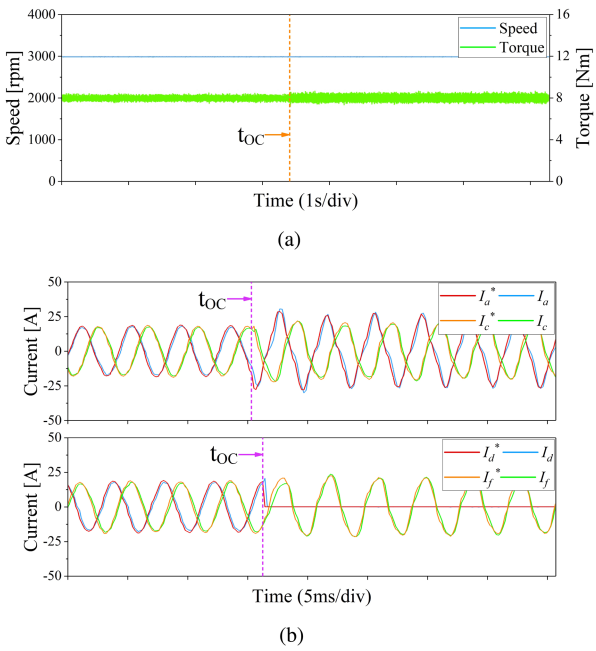

Fig. 11. Control performance under POC fault condition.

EMF feedforward compensation to obtain the better phase current control performance. Third, the systematic design method and parameter design criteria for our proposed control have been conducted, which makes it easily applied.

V. Experiment Validation

To validate the effectiveness of the proposed current control, the six-phase FTPMSM experimental platform is established as shown in Fig. 10, in which the DSP (TMS320F28335) and FPGA (EP2C35F484)-based digital controller is adopted. The motor parameters are listed in Table I. The sample frequencies for the speed loop and current loop are 15 and 20 kHz, while the PWM switching frequency is set as 20 kHz.

A. POC Fault-Tolerant Operation Condition

Fig. 11 shows the control performance of the FTPMSM system at 3000 r/min and 8 N · m under POC fault-tolerant operation condition, while the F-phase fault occurs at t_{OC}. Note that the phase currents of the FTPMSM system in normal condition are all sinusoidal with the fundamental period of 4 ms, while the nonfault phase currents are all nonsinusoidal by the fault tolerant control. Furthermore, the current tracking error the nonfault

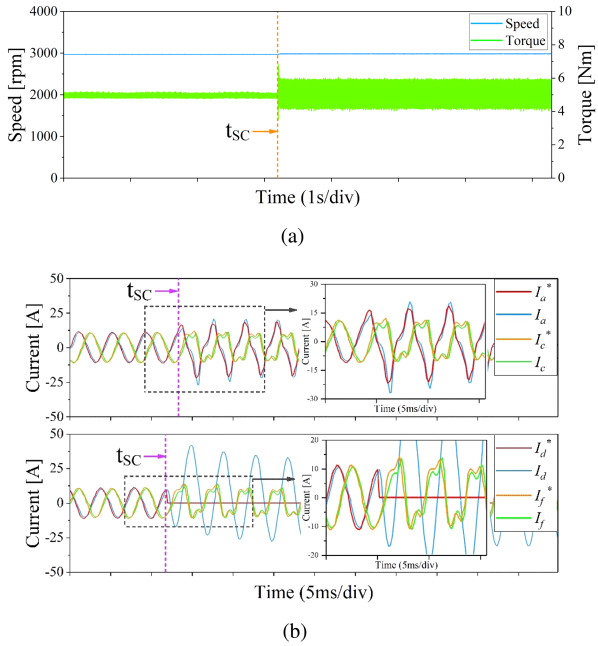

Fig. 12. Control performance under PSC fault condition.

phase currents with the proposed current control can enter a small region around zero in no more than two current periods. Therefore, the FTPMSM system under POC fault condition has the excellent control performance with almost no torque ripple.

B. PSC Fault-Tolerant Operation Condition

Fig. 12 shows the fault-tolerant control performance of the FTPMSM system at 3000 r/min and 5 N · m under PSC fault condition. Note that although the nonfault phase currents are seriously distorted after the PSC fault occurrence, the proposed current control can guarantee the phase current tracking performance. In addition, due to the existence of the short-circuit current in faulted F-phase, there is a little torque ripple for the FTPMSM during fault tolerant operation. However, the fault tolerant control performance can be still guaranteed for the FTPMSM system.

C. Speed Command Step Condition

Fig. 13 shows the speed command step response from 2000 to 3000 r/min for the FTPMSM system during the fault tolerant operation. Note that during the transient process after the speed command step occurrence, the amplitude and frequency of the nonfault phase currents will increase, while there exists a little current tracking error. As the motor speed approaches the speed command, the proposed current control can eliminate the current tracking error. Therefore, the proposed current control has the outstanding current tracking performance in the speed command step condition regardless of POC fault and PSC fault.

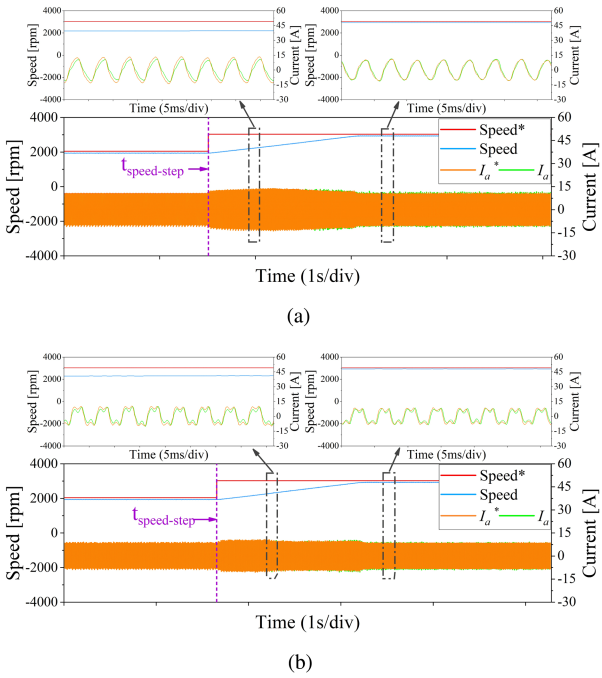

Fig. 13. Speed step response performance during fault-tolerant operation.

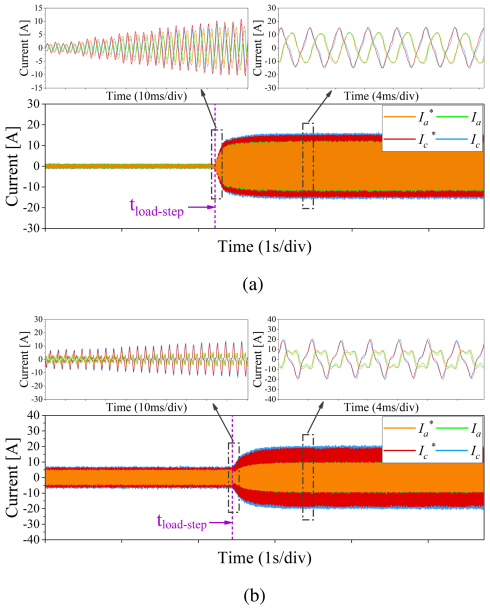

Fig. 14. Load torque step response performance during fault-tolerant operation.

D. Load Torque Step Condition

Fig. 14 shows the load torque step response from no load to 5 N · m for the FTPMSM system during the POC and PSC fault-tolerant operation. After the load torque step occurrence, the nonfault phase current of the FTPMSM will increase rapidly. By the proposed current control, the phase current tracking error can be always kept around zero. Therefore, the proposed current control has the good dynamic performance and strong robustness to the load torque step.

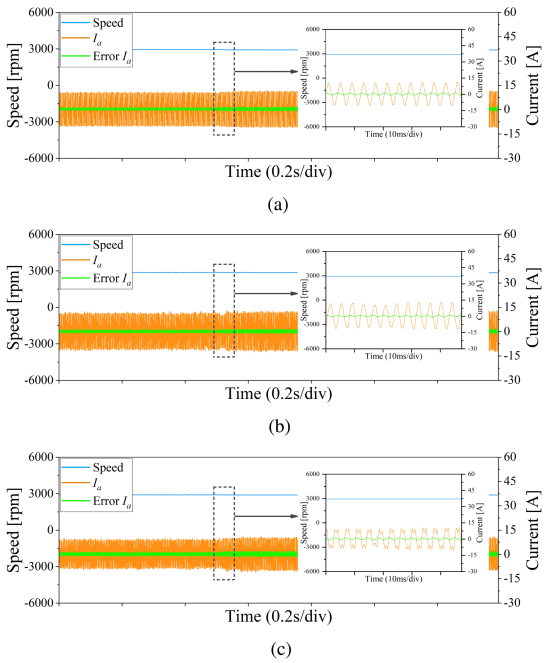

Fig. 15. Motor parameter change response performance during fault-tolerant operation.

E. Parameter Variation Condition

Fig. 15 shows the control performance of the FTPMSM system at 3000 r/min with the motor parameter variation. Here, the phase resistance changes from the nominal value (0.055 Ω) to 145% (0.08 Ω) of its nominal value, while the phase inductance changes from the nominal value (1.14 mH) to 126% (1.44 mH) of its nominal value. Note that by the phase resistance and inductance step change, although there exists a little current tracking error, the nonfault phase current tracking performance can be guaranteed with the proposed current control. Therefore, the proposed current control has good robustness to the motor parameter variation.

Note that the proposed multifrequency QPR current control has an excellent current tracking performance for the FTPMSM system, regardless of the POC/PSC fault and various disturbances. There exists little current tracking error, which may be due to the high-order harmonic current components and the time delay of the digital implementation.

VI. Conclusion

This article proposes a new fault-tolerant current control with multifrequency QPR control and back EMF feedforward compensation for the six-phase FTPMSM system, which can track the time-varying sinusoidal and nonsinusoidal reference currents in SRF under normal and POC/PSC fault conditions. To guarantee the phase current control performance over the entire operating speed range, the multifrequency QPR current

control with shunt topology is proposed, which can achieve almost no steady-state error even in a fault condition. Then the back EMF feedforward compensation approach is proposed to further enhance the current tracking performance, which takes the time delay of the digital implementation into consideration. The resulting six-phase FTPMSM system with the proposed current control has excellent current tracking performance, strong robustness to various external/internal disturbances, as well as low computational burden, which can guarantee the FTPMSM system performance in normal and fault conditions.

The novelty of this article is to propose a systematic design method of time-varying nonsinusoidal current tracking control in a stationary reference frame with the back EMF feedforward compensation. Furthermore, the proposed method is a universal current control method, which can also be generalized for other-type FTPMSM system. In addition, to achieve no static error tracking control in full-speed range, further explorations on the repetitive control-based current control for the FTPMSM system is also interesting and worth pursuing.

REFERENCES

[1] B. Sarlioglu and C. T. Morris, "More electric aircraft: Review, challenges,and opportunities for commercial transport aircraft," *IEEE Trans. Transp. Electrific.*, vol. 1, no. 1, pp. 54–64, Jun. 2015.

[2] G. Buticchi, S. Bozhko, M. Liserre, P. Wheeler, and K. A. Haddad, "On-board microgrids for the more electric aircraft—technology review," *IEEE Trans. Ind. Electron.*, vol. 66, no. 7, pp. 5588–5599, Jul. 2019.

[3] J. Q. Xu, Y. Du, B. Zhang, H. Fang, H. Guo, and Y. H. Chen, "Sensorless fault-tolerant control with phase delay compensation for aerospace FTPMSM drives with phase open-circuit and short-circuit faults," *IEEE Trans. Ind. Electron.*, vol. 68, no. 6, pp. 4576–4585, Jun. 2021.

[4] Y. Shang et al., "A novel electro hydrostatic actuator system with energy recovery module for more electric aircraft," *IEEE Trans. Ind. Electron.*, vol. 67, no. 4, pp. 2991–2999, Apr. 2020.

[5] M. T. E. Heinrich, F. Kelch, P. Magne, and L. Emadi, "Regenerative braking capability analysis of an electric taxiing system for a single aisle midsize aircraft," *IEEE Trans. Transp. Electrific.*, vol. 1, no. 3, pp. 298–307, Oct. 2015.

[6] Y. Fan, R. Cui, and A. Zhang, "Torque ripple minimization for inter-turn short-circuit fault based on open-winding five phase FTFSCW-IPM motor for electric vehicle application," *IEEE Trans. Veh. Technol.*, vol. 69, no. 1, pp. 282–292, Jan. 2020.

[7] T. Tao, W. Zhao, Y. He, Y. Cheng, S. Saeed, and J. Zhu, "Torque ripple minimization for inter-turn short-circuit fault based on open-winding five phase FTFSCW-IPM motor for electric vehicle application," *IEEE Trans. Power Electron.*, vol. 36, no. 3, pp. 3236–3246, Mar. 2021.

[8] W. Huang, W. Hua, F. Chen, M. Hu, and J. Zhu, "Model predict torque control with SVM for five-phase PMSM under open-circuit fault condition," *IEEE Trans. Power Electron.*, vol. 35, no. 5, pp. 5531–5540, May 2019.

[9] H. Guo, J. Q. Xu, and Y. H. Chen, "Robust control of fault-tolerant permanent-magnet synchronous motor for aerospace application with guaranteed fault switch process," *IEEE Trans. Ind. Electron.*, vol. 62, no. 12, pp. 7309–7321, Dec. 2015.

[10] L. F. Zhang, K. Wang, H. Y. Sun, and S. S. Zhu, "Multiphase PM machines with Halbach array considering third harmonic flux density," *IEEE Trans. Ind. Electron.*, vol. 66, no. 12, pp. 9184–9193, Dec. 2019.

[11] J. Q. Xu, Y. Du, H. Fang, H. Guo, and Y. H. Chen, "A robust observer and nonorthogonal PLL-based sensorless control for fault-tolerant permanent magnet motor with guaranteed postfault performance," *IEEE Trans. Ind. Electron.*, vol. 67, no. 7, pp. 5959–5970, Jul. 2020.

[12] A. Mohammadpour and L. Parsa, "Global fault-tolerant control technique for multiphase permanent-magnet machines," *IEEE Trans. Ind. Appl.*, vol. 51, no. 1, pp. 178–186, Jan./Feb. 2015.

[13] Z. Sun, J. Wang, G. W. Jewell, and D. Howe, "Enhanced optimal torque control of fault-tolerant PM machine under flux-weakening operation," *IEEE Trans. Ind. Electron.*, vol. 57, no. 1, pp. 344–353, Jan. 2010.

[14] G. Liu, Z. Lin, W. Zhao, Q. Chen, and G. Xu, "Third harmonic current injection in fault-tolerant five-phase permanent-magnet motor drive," *IEEE Trans. Power Electron.*, vol. 33, no. 8, pp. 6970–6979, Aug. 2018.

[15] Y. Sui, P. Zheng, Z. Yin, and C. Wang, "Open-circuit fault-tolerant control of five-phase PM machine based on reconfiguring maximum round magnetomotive force," *IEEE Trans. Ind. Electron.*, vol. 66, no. 1, pp. 48–59, Jan. 2019.

[16] A. Mohammadpour, S. Sadeghi, and L. Parsa, "A generalized fault-tolerant control strategy for five-phase PM motor drives considering star, pentagon, and pentacle connections of stator windings," *IEEE Trans. Ind. Electron.*, vol. 61, no. 1, pp. 63–75, Jan. 2014.

[17] W. Wang, J. Zhang, and M. Cheng, "A dual-level hysteresis current control for one five-leg VSI to control two PMSMs," *IEEE Trans. Power Electron.*, vol. 32, no. 1, pp. 804–814, Jan. 2017.

[18] Q. Chen, W. Zhao, G. Liu, and Z. Lin, "Extension of virtual-signal-injection-based MTPA control for five-phase IPMSM into fault-tolerant operation," *IEEE Trans. Ind. Electron.*, vol. 66, no. 2, pp. 944–955, Feb. 2019.

[19] F. Baudart, B. Dehez, E. Matagne, D. T. Nedelcu, P. Alexandre, and F. Labrique, "Torque control strategy of polyphase permanent-magnet synchronous machines with minimal controller reconfiguration under open-circuit fault of one phase," *IEEE Trans. Ind. Electron.*, vol. 59, no. 6, pp. 2632–2644, Jun. 2012.

[20] T. Tao, W. Zhao, Y. He, Y. Cheng, S. Saeed, and J. Zhu, "Enhanced fault-tolerant model predictive current control for a five-phase PM motor with continued modulation," *IEEE Trans. Power Electron.*, vol. 36, no. 3, pp. 3236–3246, Mar. 2021.

[21] H. Guzman, M. J. Duran, F. Barrero, B. Bogado, and S. Toral, "Speed control of five-phase induction motors with integrated open-phase fault operation using model-based predictive current control techniques," *IEEE Trans. Ind. Electron.*, vol. 61, no. 9, pp. 4474–4484, Sep. 2014.

[22] D. Ye, J. Li, J. Chen, R. Qu, and L. Xiao, "Study on steady-state errors for asymmetrical six-phase permanent magnet synchronous machine fault-tolerant predictive current control," *IEEE Trans. Power Electron.*, vol. 35, no. 1, pp. 640–651, Jan. 2020.

[23] W. Huang, W. Hua, F. Chen, and J. Zhu, "Enhanced model predictive torque control of fault-tolerant five-phase permanent magnet synchronous motor with harmonic restraint and voltage preselection," *IEEE Trans. Ind. Electron.*, vol. 67, no. 8, pp. 6259–6269, Aug. 2020.

[24] B. Sen and J. Wang, "Stationary frame fault-tolerant current control of polyphase permanent-magnet machines under open-circuit and short-circuit faults," *IEEE Trans. Power Electron.*, vol. 31, no. 7, pp. 4684–4696, Jul. 2016.

[25] D. Zhu, X. Zou, S. Zhou, W. Dong, Y. Kang, and J. Hu, "Feedforward current references control for DFIG-based wind turbine to improve transient control performance during grid faults," *IEEE Trans. Energy Conver.*, vol. 33, no. 2, pp. 670–681, Jun. 2018.

[26] H. Guo, J. Q. Xu, and X. Kuang, "A novel fault tolerant permanent magnet synchronous motor with improved optimal torque control for aerospace application," *Chin. J. Aeronaut.*, vol. 28, no. 2, pp. 535–544, Apr. 2015.

[27] J. B. Wang, K. Atallah, and D. Howe, "Optimal torque control of fault tolerant permanent magnet brushless machine," *IEEE Trans. Magn.*, vol. 39, no. 5, pp. 2962–2964, Sep. 2002.

[28] Y. Hu, Z. Q. Zhu, and K. Liu, "Current control for dual three-phase permanent magnet synchronous motors accounting for current unbalance and harmonics," *IEEE J. Emerg. Sel. Top. Power Electron.*, vol. 2, no. 2, pp. 272–284, Jun. 2014.

Jinquan Xu (Senior Member, IEEE) received the B.S. and Ph.D. degrees in electrical engineering from the School of Automation Science and Electrical Engineering, Beihang University, Beijing, China, in 2009 and 2015, respectively.

From 2012 to 2013, he was a Visiting Scholar with George W. Woodruff School of Mechanical Engineering, Georgia Institute of Technology, Atlanta, GA, USA. He is currently an Associate Professor with the School of Automation Science and Electrical Engineering, Beihang University His research interests include fault-tolerant permanent magnet motor systems, position sensorless control of fault-tolerant motors, fault diagnosis, and robust control.

Si Guo (Student Member, IEEE) received the B.S. and M.S. degrees in 2011 and 2014, respectively, from Beihang University, Beijing, China, where he is currently working toward the Ph.D. degree with the School of Automation Science and Electrical Engineering, all in electrical engineering.

His research interests include fault diagnosis, design, and control of the fault tolerant permanent magnet motor.

Hong Guo (Senior Member, IEEE) received the B.S., M.S., and Ph.D. degrees in electrical engineering from the Harbin Institute of Technology, Heilongjiang, China, in 1988, 1991, and 1994, respectively.

He is currently a Professor with the School of Automation Science and Electrical Engineering, Beihang University, Beijing, China. His research interests include design and control of permanent magnet motor, robust design theory and method of electrical machine, and design theory, and method of electrical machine with high reliability.

Xinlei Tian (Student Member, IEEE) received the B.S. degree in automation specialty from the University of Science and Technology Beijing, Beijing, China, in 2017, and the M.S. degree in electrical engineering in 2020 from Beihang University, Beijing, China, where he is currently working toward the Ph.D. degree in electrical engineering from the School of Automation Science and Electrical Engineering.

His research interests include fault diagnosis and tolerant control of the multiphase permanent magnet synchronous motor.